Vol. 16, No. 47, Summer 2026, pages 39-48

Journal of Analytical and Numerical Methods in Mining Engineering

Journal home page: http://anm.yazd.ac.ir/

Research Article

Slope stability analysis of Sefidabeh antimony open-pit walls

Mohamad Javad Azinfar[1*], Seyed Amirasad Fatemi[1], Soheil Zaremotlagh[1]

1- Dept. of Mining Engineering, Faculty of Engineering, University of Sistan and Baluchestan, Iran

*Corresponding author: E-mail: *j.azinfar@eng.usb.ac.ir*

(Received: *17 September 2025*, Revise: *22 November 2025*, Accepted: *13 January 2026*)

DOI: *10.22034/ANM.2026.23678.1698*

Keywords

Slope stability
Sefidabeh antimony mine
SMR
Numerical modeling
FLAC 2D
Open-pit mine slope design
Geotechnical modeling
Rock mass characterization

Abstract

In this study, the wall slope stability of the Sefidabeh antimony open-pit mine has been investigated. According to the geometry of the mining pit, three areas of the northern, middle, and southern pits have been considered, and each of them has been divided into the walls of the eastern, western, northern, and southern walls (A total of 8 walls have been examined). The geometric and mechanical characteristics of more than 500 rock joints have been surveyed in the entire mining pit area. Then, using the surveyed characteristics of the rock mass, the SMR rating of each wall was calculated, and the required stabilization measures were proposed based on it. Based on the results of the SMR rating, the walls of the middle pits and the eastern walls of the northern and southern pits need local improvement. Then, the rock mass of the walls was modeled and analyzed using FLAC 2D software. Based on the modeling results, the safety factor of all walls was found to be between 2.78 and 4.88, which, considering a minimum safety factor of 1.3 for the stability of the walls, indicates that all the mine walls are currently stable. Finally, assuming a GSI = 50, the lowest geological strength index surveyed from the walls, a sensitivity analysis of the slopes was performed with respect to changes in the overall slope angle, the height of the walls (mine depth), and changes in the compressive strength of the rocks. The results are presented in the form of graphs.

1. INTRODUCTION

Determining the slope of open-pit mine walls is one of the most important parameters in mining design. If the slope of the walls is considered low, the stripping ratio will increase significantly. On the other hand, choosing steeper walls will reduce safety and increase the possibility of failures. Therefore, choosing the optimal slope is necessary to prevent the excess stripping ratio and reduce the risk of wall failures. In addition, assigning a slope to the entire mine wall is not correct in most mines because the mine walls are usually made of different materials and with different structural conditions. Therefore, the slope design should be determined after determining the geotechnical parameters, different lithologies, and identifying the geotechnical limits of the mining pit. There are different methods for analyzing the stability of the slope of open-pit walls. Among them are empirical methods, limit equilibrium methods, and numerical methods.

One of the most important issues in slope design in most open-pit mines is determining the failure mechanism. The rock mass forming each rock slope has unique characteristics depending on the scale of the operation. The wall height, geological conditions, rock strength, groundwater status, and mine blasting conditions are among the factors affecting the stability of the slope and mine walls. By considering geological data, geomechanical information, groundwater status observation, and sound engineering judgment, a scientific solution can be provided for this issue.

The selection of slope stability analysis methods for different mines depends on the depth and age of the mine, the rock type, and the main geological structures of the area, and the stage of the project. The deeper the mine and the age, the more complex the geological conditions of the area, and the more advanced the project stage, the more accurate the stability analysis should be performed. The engineering judgment plays the most important role in selecting the method [1].

In the present study, the empirical methods of rock mass rating (RMR) [2] and SMR [3], and numerical modeling with FLAC 2D software were used to analyze the stability of the walls of the Sefidabeh antimony mine. The innovation of this research is the sensitivity analysis of the stability of mine walls to changes in wall height in the mine development plan, changes in wall slope to optimize the stripping ratio, and changes in the uniaxial compressive strength of the rocks.

1.1. Geological Conditions And Mine Location

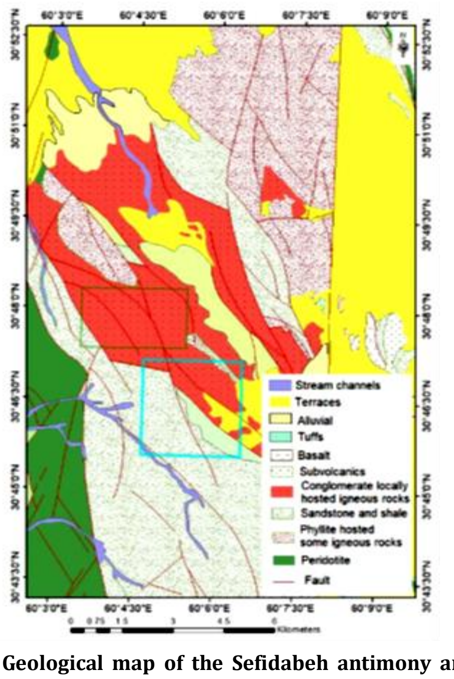

Fig. 1. Geological map of the Sefidabeh antimony areas, modified from the geological map of 100,000 Siastragi. The blue squares indicate the Sefidabeh area and the green squares indicate the Hyderabad area [5].

The Sefidabeh antimony deposit is located about 280 km northwest of Zahedan. Figure 1 shows the geology of the Sefidabeh and Hyderabad areas on the 1:100,000 geological map of the Siastragi Mountains. According to this geology map, the rocks in mine area and its surroundings in this map are ophiolitic, turbiditic, and felsic complexes, and volcanic and subvolcanic igneous rocks. In the eastern part, the flysch has been metamorphosed and transformed into phyllite and slate. In the western part, the sedimentary rocks are mainly turbiditic. All the boundaries between the complexes and units of rocks are faulted, and in fact, the mineral area is a shear zone with many intersecting faults. The turbiditic and flysch complex is the most extensive rock complex in the region, where antimony mineralization has also occurred. The flysch and turbidite complexes in the area consist of various rock units and sequences, mainly including conglomerate, sandstone, shale, siltstone, and, less often, mudstone and rarely limestone, which have various colors and are sometimes altered.

The study area is located between two main strike-slip faults, the "East Neh" fault and the "West Asagi" fault, and is strongly affected by these faults [4]. The current area of the Sefidabeh antimony mine pit is located within the UTM coordinates of R41 221800E-3407900N and R41 222000E-3408275N. The stibnite veins in the mine were first observed by local people in the outcrop, and then the investigation, exploration, and extraction were carried out by several companies. Since 2021, the IMPASCO (Iran Mineral Production and Supply Company) has entrusted the implementation of operations related to exploration, equipping, preparation, waste removal, and extraction of minerals from the Sefidabeh mine and several other antimony mines in Sistan and Baluchestan province to the Golgohar Mining and Industrial Company for a period of 10 years. The map of the mine pits is shown in Figure 2.

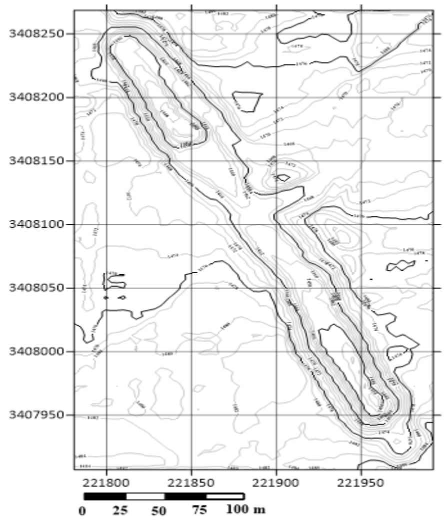

Fig. 2. Areas of the southern, middle, and northern pits of the Sefidabeh antimony mine.

2. DETERMINING THE MAJOR JOINT SETS IN THE MINE AREA

In the geotechnical survey of the mine area, more than 500 rock joints were surveyed, and their geometric and mechanical characteristics were collected. The direction and slope of the joints and faults were measured with a compass. For this purpose, the area survey method (window) with window dimensions of 10×10 meters was used. Considering the environment of the mine pit floor, 63 windows were surveyed at the level of the last steps. On average, 2 to 3 joints were surveyed from each joint set in each window. With the increase in the mine environment at higher levels, the dimensions of the survey windows increased to keep the same number of 63 windows constant. The northern pit is divided into three walls: eastern (NP-EW), western (NP-WW), and northern (NP-NW); the southern pit is divided into three walls: eastern (SP-EW), western (SP-WW), and southern (SP-SW); and the middle pit is divided into two walls: eastern (MP-EW) and western (MP-WW) (Figure 3). The characteristics of the major joint sets for the entire mine area were obtained using Dips software and are shown in Figure 4. Given that each of the mine walls is analyzed separately in the following, the major joint sets for each wall are also obtained separately and are presented in Table 1. Between two and three major joint sets have been identified in different walls.

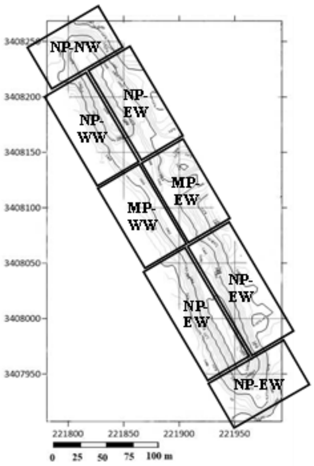

Fig. 3. Location of the named pit walls of the mine.

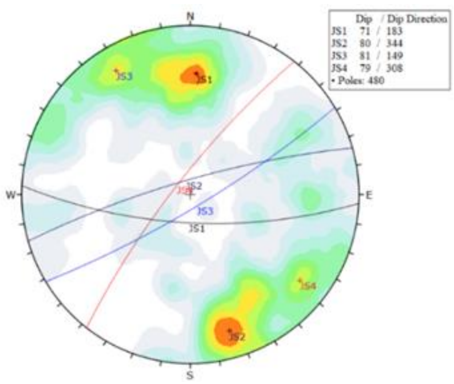

Fig. 4. Major joint set in the mining pits.

Table 1. Characteristics of the joint sets surveyed in each wall

Mining pit	Wall	Joint sets (Dip / Dip Direction)
North Pit (NP)	NP-EW	JS1: 72 / 181 JS2: 70 / 329 JS3: 72 / 82
	NP-NW	JS1: 67 / 258 JS2: 64 / 230
	NP-WW	JS1: 85 / 343 JS2: 68 / 179 JS3: 75 / 239
Middle pit (MP)	MP-EW	JS1: 77 / 303 JS2: 79 / 334 JS3: 87 / 115
	MP-WW	JS1: 88 / 117 JS2: 57 / 349 JS3: 33 / 65
South Pit (SP)	SP-EW	JS1: 73 / 347 JS2: 70 / 272 JS3: 55 / 188
	SP-SW	JS1: 84 / 347 JS2: 81 / 188 JS3: 11 / 80
	SP-WW	JS1: 80 / 148 JS2: 35 / 14 JS3: 71 / 240

3. ANALYSIS OF MINE WALL SLOPE STABILITY USING THE SMR METHOD

The SMR system is based on the RMR classification system and in this system, in addition to the basic parameters of the RMR_{Basic} system [6], which include the strength of the intact rock (A), RQD (B), and spacing (C), condition (D) and water status (E) in the discontinuities (Equation 1), it also includes the spatial location of the discontinuities relative to the slope and the method of excavation of the steps [3]. The SMR classification has been used in various slope stability projects around the world for the past few decades [7].

$$RMR = A + B + C + D + E \tag{1}$$

The method of determining the RMR_{Basic} rating is presented by Bieniawski in the form of relevant tables [6]. After calculating the basic RMR, the SMR rating is expressed by Eq. (2):

$$SMR = RMR_{basic} + (F_1F_2F_3) + F_4 \tag{2}$$

where F_1 represents the parallelism between the direction of the dominant discontinuity slope α_j and the direction of the wall slope α_s. This coefficient varies from 1 for the case where both are almost parallel to 0.15 for the case where the angle between them is greater than 30 degrees, and the probability of failure is very low. The value of F_1 is determined from Eq. (3):

$$F_1 = (1 - sin\,\alpha)^2 \tag{3}$$

In this relation, $\boldsymbol{\alpha}$ is the angle between the direction of the dominant discontinuity slope α_j and the direction of the wall slope α_s. The different values of F_1, F_2, and F_3 are presented in Table 2.

Table 2. Different values of F1, F2, and F3 in the context of different joint orientations [8]

Type of failure		Very favorable	Favorable	Fair	Unfavorable	Very unfavorable
P	$\lvert\alpha_j - \alpha_s\rvert$	> 30°	20–30°	10–20°	5–10°	< 5°
T	$\lvert\alpha_j - \alpha_s - 180\rvert$					
W	$\lvert\alpha_i - \alpha_s\rvert$					
P/W/T	F_1	0.15	0.4	0.7	0.85	1
P	β_j	< 20°	20–30°	30–35°	35–45°	> 45°
W	β_i					
P/W	F_2	0.15	0.4	0.7	0.85	1
T	F_2	1	1	1	1	1
P	$\lvert\beta_j - \beta_s\rvert$	>10°	0–10°	0°	−10–0°	< −10°
W	$\lvert\beta_i - \beta_s\rvert$					
T	$\beta_j + \beta_s$	<110°	110–120°	>120°	--	--
P/W/T	F_3	0	-6	-25	-50	-60

The initial table presented by Romana [3] included planar and toppling failure, and Anbalagan et al. [8] also added the values of F_1 for wedge failure. The P, T, and W failures mean planar, toppling, and wedge failure, respectively, and α_i and β_i are the direction angle and slope angle of the intersection of the two dominant discontinuities in the wedge failure, respectively. The value of F_2 is related to the slope angle of the dominant joint in the case of planar failure or the angle of the intersection of the two dominant joints in the case of wedge failure. The size of this coefficient varies from 0.15 to 1 (for toppling failure) and is obtained from the following equation.

$$F_2 = tan^2 \beta_j \quad (4)$$

In this relation, β_j is the slope angle of the dominant discontinuity. In the case of a wedge failure, β_i is used in this equation. The value of F_3 depends on the relationship between the wall slope β_s and the dominant discontinuity slope β_j. In the case of a wedge failure, β_i is used instead of β_j in this equation. The value of F_4 is the coefficient related to the excavation method, the values of which are shown in Table 3.

Table 3. Empirical values for the excavation method [1]

Excavation method	F_4 values
Natural slope	+15
Presplitting	+10
Smooth blasting	+8
Blasting or Mechanical	0
Deficient blasting	-8

To examine the stability of the mine walls, the basic RMR values were initially calculated for each of the 8 walls. The wall slopes were calculated using the sections drawn on the mine topographic map using Surfer and Geomagic Studio software. The coefficient F_4 is considered zero for both failure modes, considering that the mining is carried out mechanically (by hydraulic hammer). Table 4 shows the calculated SMR rating for the different mine walls.

Based on the SMR rating in the plane and toppling failure, the rock mass stability conditions of the different walls and the proposed stabilization system are shown in Table 5. Among the results obtained for SMR in Table 4 for different joint sets, the more critical SMR values are considered. According to Table 5, most of the walls are in a normal state in terms of rock mass conditions. These walls may need local rock mass improvement. The walls of the middle pits (MP-EW and MP-WW) and the eastern walls of the northern and southern pits (NP-EW and SP-EW) are in this state. Only the western wall of the northern pit (NP-WW), due to the presence of joint set number 3, is in an unstable condition in terms of toppling failure, which requires special stabilization measures based on the items proposed in Table 5. Of course, the aforementioned wall has an SMR rating of 62 in terms of plane failure and is in good rock mass condition.

Table 4. Calculation of SMR rating for different mine walls

Mine wall	Joint Sets	RMR	αj	αs	βj	βs	F1 (P)	F2 (P)	F3 (P)	F1 (T)	F2 (T)	F3 (T)	SMR (P)	SMR (T)
MP-EW	JS1	57	303	242	77	32	0.15	1	0	0.15	1	0	57	57
	JS2	57	334	242	79	32	0.15	1	0	0.15	1	-6	57	56
	JS3	57	115	242	87	32	0.15	1	0	0.15	1	-6	57	56
NP-EW	JS1	58	181	240	72	41	0.15	1	0	0.15	1	-6	58	57
	JS2	58	329	240	70	41	0.15	1	0	0.15	1	-6	58	57
	JS3	58	82	240	72	41	0.15	1	0	0.15	1	-6	58	57
NP-NW	JS1	60	258	123	67	41	0.15	1	0	0.15	1	0	60	60
	JS2	60	230	123	64	41	0.15	1	0	0.15	1	0	60	60
NP-WW	JS1	62	343	56	85	49	0.15	1	0	0.15	1	-25	62	58
	JS2	62	179	56	68	49	0.15	1	0	0.15	1	-6	62	61
	JS3	62	239	56	75	49	0.15	1	0	1	1	-25	62	37
MP-WW	JS1	55	117	36	88	31	0.15	1	0	0.15	1	-6	55	54
	JS2	55	349	36	57	31	0.15	1	0	0.15	1	0	55	55
	JS3	55	65	36	33	31	0.4	0.42	-6	0.15	1	0	54	55
SP-WW	JS1	61	148	54	80	48	0.15	1	0	0.15	1	-25	61	57
	JS2	61	14	54	35	48	0.15	0.49	-60	0.15	1	0	56	61
	JS3	61	240	54	71	48	0.15	1	0	0.85	1	-6	61	55
SP-SW	JS1	68	347	217	84	33	0.15	1	0	0.15	1	-6	68	67
	JS2	68	188	217	81	33	0.4	1	0	0.15	1	-6	68	67
	JS3	68	80	217	11	33	0.15	0.15	-60	0.15	1	0	66	68
SP-EW	JS1	61	347	237	73	47	0.15	1	0	0.15	1	-25	61	57
	JS2	61	272	237	70	47	0.15	1	0	0.15	1	-6	61	60
	JS3	61	188	237	55	47	0.15	1	-6	0.15	1	0	60	61

Table 5. Proposed stabilization measures for different mine walls based on SMR rating

Mine wall	SMR (P/T)	SMR Rating	Description of rock mass	Stability	Failure	Failure probability	Proposed stabilization
MP-EW	SMR (P)	57	Normal	Partially stable	Planar along some joints and wedges	40%	Toe or Slope fences, Anchors, Bolts, Shotcrete
	SMR (T)	56	Normal	Partially stable			
NP-EW	SMR (P)	58	Normal	Partially stable			
	SMR (T)	57	Normal	Partially stable			
NP-NW	SMR (P)	60	Normal	Partially stable			
	SMR (T)	60	Normal	Partially stable			
NP-WW	SMR (P)	62	Good	Unstable	Some blocky failure	20%	Toe or Slope fences, Anchors, Bolts
	SMR (T)	37	Bad	Unstable	Toppling	60%	Bolts, Shotcrete, Toe walls, Dental concrete, Surface drainage
MP-WW	SMR (P)	54	Normal	Partially stable	Planar along some joints and wedges	40%	Toe or Slope fences, Anchors, Bolts, Shotcrete
	SMR (T)	54	Normal	Partially stable			
SP-WW	SMR (P)	56	Normal	Partially stable			
	SMR (T)	55	Normal	Partially stable			
SP-SW	SMR (P)	66	Good	Unstable	Some blocky failure	20%	Toe or Slope fences, Anchors, Bolts
	SMR (T)	67	Good	Unstable			
SP-EW	SMR (P)	60	Good	Unstable			
	SMR (T)	57	Normal	Partially stable	Planar along some joints and wedges	40%	Toe or Slope fences, Anchors, Bolts, Shotcrete

4. ANALYZING THE STABILITY OF WALLS USING NUMERICAL METHODS

In order to perform more accurate analyses of the slope stability of the mine walls, in this research, considering the number of joint sets in the rock mass, was used the continuum numerical method by FLAC 2D software.

To determine the mechanical properties of the models (such as E_m, m_b, and S), empirical methods such as RMR, Q, and GSI have been used [9-13]. The estimated values of the rock mass deformation modulus by Serafim [9], Barton et al. [10], and Bieniawski [11] for different walls range from 10 to 29 GPa, which are much higher than the average Young's modulus obtained from intact rock samples in the laboratory (5.82 GPa). Therefore, in this study, the average of Eq. (5) and (6), which are related to references [12] and [13] and are more up-to-date than the other relations presented, has been used.

$$E_m\,(GPa) = \left(1-\frac{D}{2}\right)\sqrt{\frac{\sigma_{ci}}{100}}\,10^{\left(\frac{GSI-10}{40}\right)} \quad \sigma_{ci} \le 100 \tag{5}$$

$$E_m\,(GPa) = \left(1-\frac{D}{2}\right)10^{\left(\frac{GSI-10}{40}\right)} \quad \sigma_{ci} > 100$$

$$E_m = E_i\left(0.02 + \frac{1-D/2}{1+e^{\left(\frac{60+15D-GSI}{11}\right)}}\right) \tag{6}$$

where σ_{ci}, D, and E_i are the uniaxial compressive strength of the rock, the value corresponding to the degree of disturbance of the rock mass, which varies between 0 and 1, and the elastic modulus of the intact rock, respectively.

To estimate the strength of the rock mass in each wall, the Hooke and Brown criterion was used, according to the relationships provided for m_b and S [14]. To determine the Poisson's ratio more accurately, Eq. (7) presented by Vasarelli was used [15].

$$\nu_{rm} = -0.002\,GSI - 0.003\,m_i + 0.457 \tag{7}$$

where m_i is the Hooke and Brown constant for intact rock.

To obtain the mechanical parameters of intact rock, the *UCS* tests were performed on 13 samples, and the average UCS and elastic modulus of intact rock after statistical corrections were 25 and 5820 MPa, respectively. Direct shear tests were also performed on the samples of the saw-cut and natural joints, and the shear and normal stiffness of the joints were obtained. The shear and normal stiffness of the natural joints were 0.6 and 2.1 MPa/mm, respectively. The numerical models of the current mine walls after plastic solving are shown in Figure 5. According to the figures, the safety factors of all walls are greater than 1.3 and the walls are stable.

Table 6. Mechanical parameters of the rock mass for different mine walls

Mine wall	RMR	GSI	E_m (GPa) (Eq. 5)	E_m (GPa) (Eq. 6)	Average E_m	m_b	S	ν_{rm}	σ_t(MPa) Rock mass	σ_c(MPa) Rock mass
MP-EW	57	52	3.646	0.71	2.178	1.359	0.001	0.3	0.018	0.745
NP-EW	58	53	3.862	0.756	2.309	1.436	0.0011	0.29	0.019	0.804
NP-NW	60	55	4.333	0.859	2.596	1.603	0.0015	0.29	0.023	0.934
NP-WW	62	57	4.862	0.974	2.918	1.789	0.002	0.29	0.027	1.084
MP-WW	55	50	3.25	0.624	1.937	1.218	0.0007	0.3	0.015	0.64
SP-WW	61	56	4.59	0.915	2.752	1.694	0.0017	0.29	0.025	1.006
SP-SW	68	63	6.869	1.386	4.127	2.488	0.0047	0.27	0.048	1.693
SP-EW	61	56	4.59	0.915	2.752	1.694	0.0017	0.29	0.025	1.006

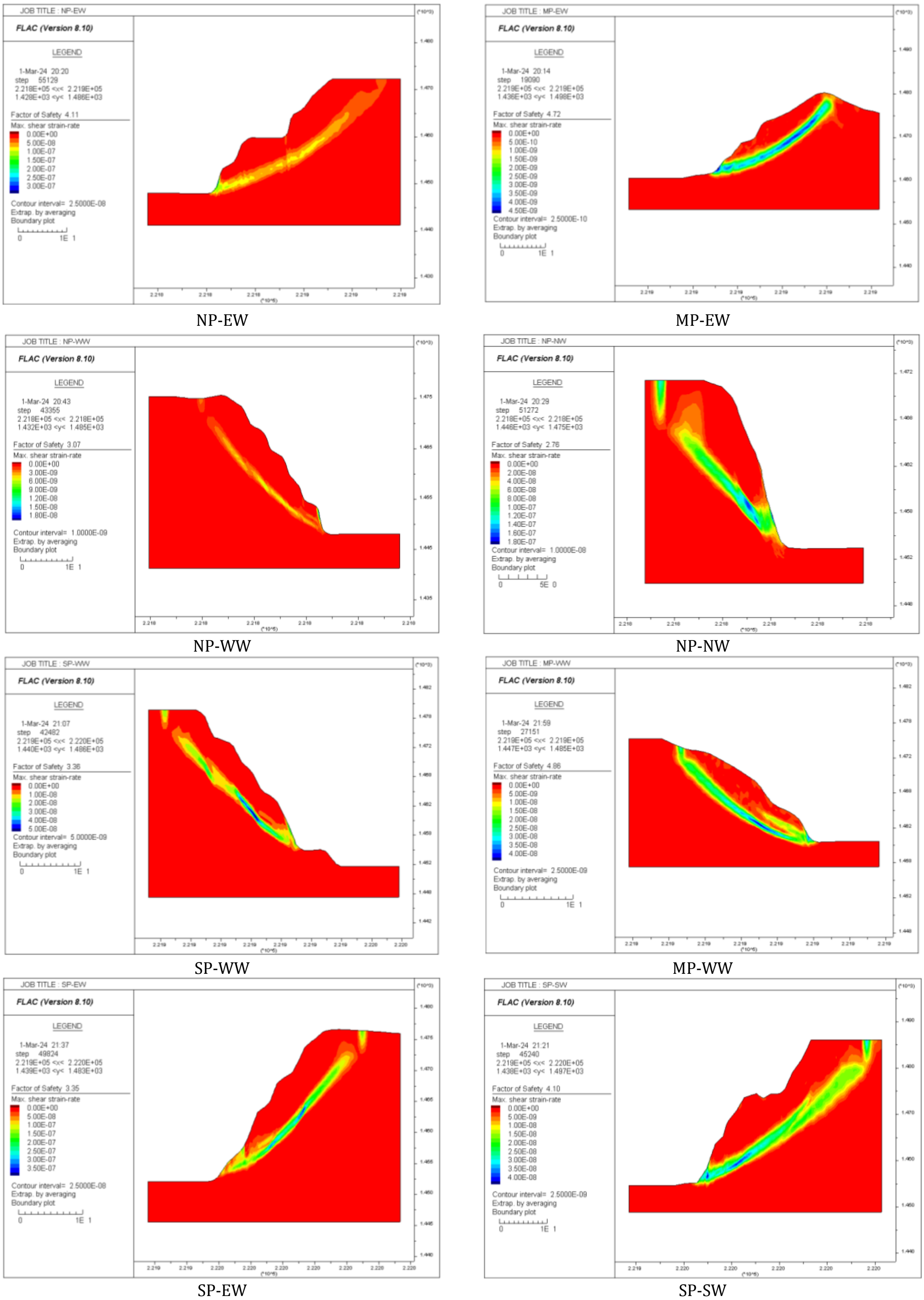

Fig. 5. Shear strain rate contour lines in different walls after plastic solving.

4.1. Sensitivity Analysis Of Wall Stabilities To Their Overall Slope

To investigate the sensitivity of the wall stabilities (safety factor) to changes in their slope, 6 slope angles of 30, 50, 40, 60, 70 and 80 degrees have been considered for models with the same height of 40 meters (Fig. 6). The height of the mine walls is currently mainly less than 30 meters and, assuming that 10 meters will be added to the mine depth soon, a height of 40 meters has been considered for stability analysis. The quality of the rock mass in all models is constant and based on the lowest GSI of the walls, which is equal to 50, with the UCS of intact rock equal to 25 MPa. The safety factor for slopes of 30 to 80 degrees has decreased from 4.32 to 1.28. Considering a safety factor of at least 1.3 for slope stability and considering a height of 40 meters, the maximum safe slope for the walls will be 80 degrees (Fig. 7).

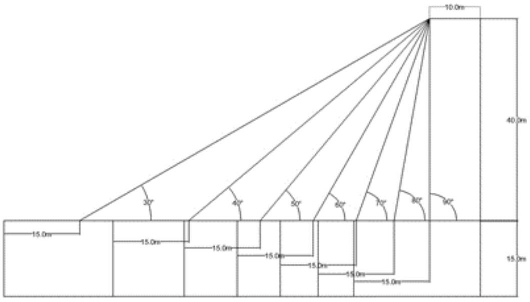

Fig. 6. Geometry of models for investigating the sensitivity analysis of the overall slope angle of the walls.

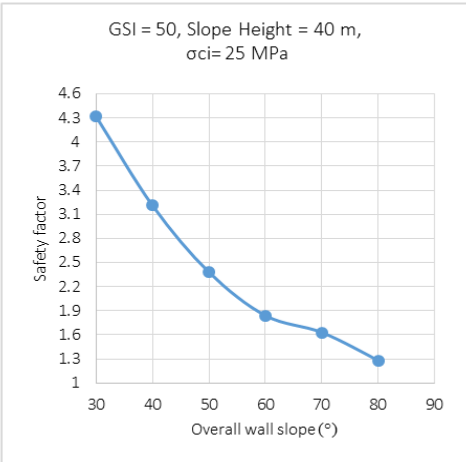

Fig. 7. Diagram of the safety factor for different wall slopes for a height of 40 meters, GSI = 50, and σ_{ci} = 25 MPa

4.2. Sensitivity Analysis Of Wall Stabilities To Their Heights

The sensitivity of wall stabilities was also investigated under the conditions that their overall slope is 70 degrees, GSI = 50, the uniaxial compressive strength of intact rock in the walls is 25 MPa, and the height of the walls varies from 15 to 65 meters (in 10-meter steps) (Fig. 8).

The safety factor has decreased from 2.74 to 1.26 from a height of 15 to 65 meters. Considering a minimum safety factor of 1.3 for slope stability considering an overall slope of 70 degrees, the maximum safe height for the walls will be approximately 58 meters (Fig. 9).

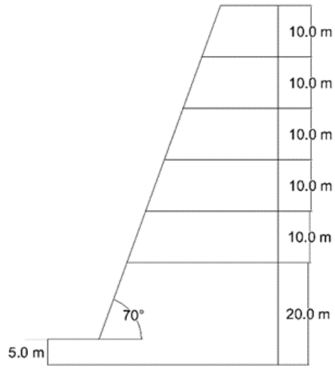

Fig. 8. Geometry of models with varying heights from 15 to 65 meters.

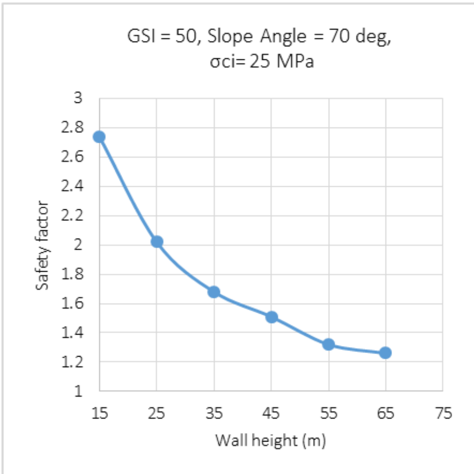

Fig. 9. Diagram of the safety factor for different wall heights with the overall slope of 70 degrees, GSI = 50, and σ_{ci} = 25 MPa.

4.3. Sensitivity Analysis Of Wall Stability To Changes In Uniaxial Compressive Strength Of Rocks

Given that UCS samples were prepared from specific points of the mine, there is a possibility of changes in this parameter in other parts of the mine. Also, the laboratory results of UCS samples were scattered, so in order to more accurately analyze the stability conditions, the stability of the walls with respect to the changes in the UCS of intact rock in numerical models was also examined. For this purpose, the wall height was 40 meters, the overall slope of the wall was 70 degrees, GSI = 50, and the values of UCS were considered to be 10, 15, 20, 30, 40, and 50 MPa according to the laboratory results.

It should be noted that in materials with strengths less than 10 MPa, several models were analyzed, in all of which, even after performing more than one million cycles, the models did not reach equilibrium in the elastic state. Therefore, strengths from 10 MPa and above are considered. By increasing the UCS of the materials from 10 to 50 MPa, the safety factor of slopes with the aforementioned specifications increases from 1.09 to 2.28 (Fig. 10).

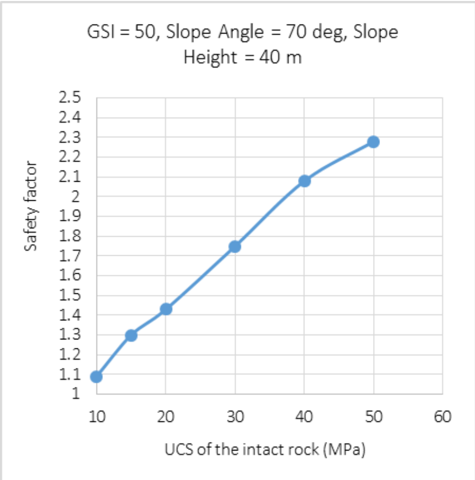

Fig. 10. Diagram of the safety factor for different uniaxial compressive strengths, with a total slope of 70 degrees and GSI = 50.

5. CONCLUSION

In the present study, the slope stability analysis of the walls of the Sefidabeh antimony mine was carried out using two empirical (SMR) and numerical (using FLAC 2D software) methods. Based on SMR ratings, most of the walls are in normal and relatively stable conditions. These walls may need to be locally stabilized. The walls of the middle pits (MP-EW and MP-WW) and the eastern walls of the northern and southern pits (NP-EW and SP-EW) are in this state. The western wall of the southern pit (SP-WW) is in better condition than the other walls and is in a stable state. Only the western wall of the northern pit (NP-WW), due to the presence of its joint set No. 3, is in an unstable condition in terms of toppling failure, which requires special stabilization measures according to Table 5.

Based on field observations, in the mine pit, the rock mass close to the earth's surface has lower ratings due to rock weathering. Therefore, safety measures and wall stabilizations should mainly be carried out in the steps located at higher levels of the mine (generally areas above 1500 meters).

In the following, the stability analysis is carried out numerically by entering the equivalent mechanical parameters of the rock mass, and the Hooke and Brown structural model is considered for the behavior of the rock mass. Initially, all the walls were modeled, and their safety factors were obtained between 2.78 and 4.88, which, considering the minimum safety factor of 1.3 for the stability of the walls in open pit mines, means all the mine walls are currently stable.

According to the mine development plan, the sensitivity analysis of the stability of the walls was also carried out with respect to changes in slope, height, and UCS of the rocks. The GSI is considered equal to 50 for all models, which is the minimum value obtained for the walls according to field surveys. To investigate the sensitivity of the stability of the walls to changes in their slope, 6 slope angles of 30 to 80 degrees were considered for models with the same height of 40 meters and a constant UCS of 25 MPa, and the maximum stable slope of the mine was 80 degrees. The sensitivity of the stability of the walls in conditions where their overall slope is 70 degrees and a constant UCS of 25 MPa with different wall heights from 15 to 65 meters was also investigated, and the maximum stable height for the slopes in this case was 58 meters. The stability of the walls to changes in the UCS of the intact rock assigned to the numerical models was also investigated. For this purpose, the height and overall slope of the walls were considered to be 40 meters and 70 degrees, respectively, and the values of UCS were considered to be between 10 and 50 MPa according to the obtained range from laboratory results. The analysis results showed that the mine wall, whose rocks have a UCS greater than 15 MPa, would be stable.

Acknowledgements

This research was supported by the respected Research and Technology Management of Golgohar Mining and Industrial Company. Therefore, the authors consider it necessary to express their gratitude to the respected managers and personnel of that company, especially Mr. Rahim Sotoudeh Bahreini, Mr. Mohammad Amiri Hosseini, and Mr. Seyyed Morteza Sajjadian.

REFERENCES

[1] Program for preparing mining standards and criteria - Ministry of Industries and Mines, Guidelines for analyzing and stabilizing slopes in open-pit mines, Deputy for Strategic Supervision of Technical System Affairs, Ministry of Industries and Mines. 2010 [In Persian].

[2] Bieniawski, Z.T., (1989), Engineering rock mass classifications: a complete manual for engineers and geologists in mining, civil, and petroleum engineering: New York, Wiley, xii, 251 p. p.

[3] Romana M., (1985). New adjustment ratings for application of Bieniawski classification to slopes, in: Proceedings of the International Symposium

on the Role of Rock Mechanics in Excavations for Mining and Civil Works. International Society of Rock Mechanics, Zacatecas, pp. 49-53 .

[4] Aghanabati, S.A., 1991. Geological map of Kuh-e-Seyasteragi (1:100000). Geological survey Of Iran.

[5] Bomari, M., Bagheri, S., Biyabangard, H., Ghodsi, M. R., (2021). Antimony mineralization controllers and its exploration routes in Sefidaba and Heydarabad and adjacent areas, Sistan Seam Zone, Sistan and Baluchestan Province, Sistan and Baluchestan University research project. 500 p. [In Persian]

[6] Bieniawski Z.T. (1973). “Engineering classification of jointed rock masses”. Trans. South Afr. Inst. of Civ. Eng. Vol. 15, N12, pp 355-344.

[7] Romana, M., Tomás, R., & Serón, J. B. (2015, May). Slope Mass Rating (SMR) geomechanics classification: thirty years review. In ISRM Congress (pp. ISRM-13CONGRESS). ISRM.

[8] Anbalagan, R., Sharma, S., & Raghuvanshi, T. K. (1992, June). Rock mass stability evaluation using modified SMR approach. In Rock mechanics proceedings of the Sixth National Symposium on Rock Mechanics (pp. 258-268).

[9] Serafim, J. L. (1983). Consideration of the geomechanical classification of Bieniawski. In Proc. int. symp. on engineering geology and underground construction (Vol. 1, pp. 33-44).

[10] Barton N, Loset F, Lien R, Lune J (1980) Application of Q-system in design decisions concerning dimensions and appropriate stabilization for underground installations. Subsurface Space, Pergamon, pp 553–561

[11] Bieniawski, Z. T. (1989). Engineering rock mass classifications: a complete manual for engineers and geologists in mining, civil, and petroleum engineering. John Wiley & Sons.

[12] Hoek, E., Carranza-Torres, C., Corkum, B., (2002), HOEK-BROWN FAILURE CRITERION – 2002 EDITION, Proceeding of the fifth North American Rock Mechanics Symposium, University of Toronto.

[13] Hoek, E., & Diederichs, M. S. (2006). Empirical estimation of rock mass modulus. International journal of rock mechanics and mining sciences, 43(2), 203-215.

[14] Hoek, E., & Brown, E. T. (1997). Practical estimates of rock mass strength. International journal of rock mechanics and mining sciences, 34(8), 1165-1186.

[15] Vásárhelyi, B. (2009) "A possible method for estimating the Poisson's rate values of the rock masses", Acta Geodaetica et Geophysica Hungarica, 44(3), pp. 313–322.

[16] Wyllie, D. C., & Mah, C. (2004). Rock slope engineering. CRC Press. 4th edition.

[17] Salu, S. P., & Bima, B. (2024). Impact Of Open-pit Mining Expansion on Slope Stability at Pt. Hikari Jeindo, Langgikima, North Konawe, Indonesia. Journal of Mining and Environment, 15(3), 943-959.”

[18] Jing, L., & Hudson, J. A. (2002). Numerical methods in rock mechanics. International Journal of Rock Mechanics and Mining Sciences, 39(4), 409-427.

[19] Xia, L., Zheng, Y., & Yu, Q. (2016). Estimation of the REV size for blockiness of fractured rock masses. Computers and Geotechnics, 76, 83-92.